Published in final edited form as:
Brain Res. 2015 February 19; 1598: 31–45. doi:10.1016/j.brainres.2014.12.016.

Frequency-Band Signatures of Visual Responses to Naturalistic Input in Ferret Primary Visual Cortex during Free Viewing

Kristin K. Sellers[1,2], **Davis V. Bennett**[1,*], and **Flavio Frohlich**[1,2,3,4,5]

[1]Department of Psychiatry, University of North Carolina at Chapel Hill, Chapel Hill NC 27599

[2]Neurobiology Curriculum, University of North Carolina at Chapel Hill, Chapel Hill NC 27599

[3]Department of Cell Biology and Physiology, University of North Carolina at Chapel Hill, Chapel Hill NC 27599

[4]Department of Biomedical Engineering, University of North Carolina at Chapel Hill, Chapel Hill NC 27599

[5]Neuroscience Center, University of North Carolina at Chapel Hill, Chapel Hill NC 27599

Abstract

Neuronal firing responses reflect the statistics of visual input and emerge from the interaction with endogenous network dynamics. Artificial visual stimuli presented to animals in which the network dynamics were constrained by anesthetic agents or trained behavioral tasks have provided fundamental understanding of how individual neurons in primary visual cortex respond to input. In contrast, very little is known about the mesoscale network dynamics and their relationship to microscopic spiking activity in the awake animal during free viewing of naturalistic visual input. To address this gap in knowledge, we recorded local field potential (LFP) and multiunit activity (MUA) in all layers of primary visual cortex (V1) of awake, freely viewing ferrets presented with naturalistic visual input (nature movie clips). We found that naturalistic visual stimuli modulated the entire oscillation spectrum; low frequency oscillations were mostly suppressed whereas higher frequency oscillations were enhanced. In average across all cortical layers, stimulus-induced change in delta and alpha power negatively correlated with the MUA responses, whereas sensory-evoked increases in gamma power positively correlated with MUA responses. The time-course of the band-limited power in these frequency bands provided evidence for a model in which naturalistic visual input switched V1 between two distinct, endogenously present activity states defined by the power of low (delta, alpha) and high (gamma) frequency oscillatory activity.

Correspondence should be addressed to: Flavio Frohlich, 115 Mason Farm Rd. NRB 4109F, Chapel Hill, NC. 27599. flavio_frohlich@med.unc.edu. Phone: 1.919.966.4584.
*Present address: Janelia Farm, Ashburn, VA 20147

Authorship Statement: KS and FF designed the experiments, KS, DB, and FF performed the experiments, KS and FF analyzed the data, and KS and FF wrote the paper.

The authors declare no competing financial interests.

Therefore, the two mesoscale activity states delineated in this study may define the engagement of the circuit with processing sensory input at the level of spiking activity.

Keywords

Primary visual cortex; naturalistic visual stimulation; ferret; cortical oscillation; free viewing; local field potential

1. Introduction

Encoding of sensory stimuli in cortex represents the process of transforming external physical signals into neuronal activity patterns that reduce the redundancy of the sensory input (Barlow, 1961; Simoncelli and Olshausen, 2001b). In primary visual cortex (V1), the responses of individual neurons and networks of neurons to synthetic visual stimuli measured by changes in action-potential firing are well characterized (Hubel and Wiesel, 1959; but see Olshausen and Field, 2005). These “artificial” stimuli have been optimized to elicit neuronal spiking responses as a function of basic input properties such as orientation, contrast, and spatial frequency. Recently, it has been proposed that synthetic stimuli modulate neuronal activity differently than naturalistic visual stimuli (Felsen and Dan, 2005; Smyth et al., 2003b) due to the different image statistics of synthetic laboratory stimuli and real-world visual input (Simoncelli and Olshausen, 2001b). Specifically, naturalistic stimuli exhibit a characteristic $1/f$ to $1/f^2$ power distribution as a function of spatial frequency f (Ruderman and Bialek, 1994; Simoncelli and Olshausen, 2001a; Tolhurst et al., 1992; van der Schaaf and van Hateren, 1996). Studies that employed naturalistic images and movie segments to investigate neuronal responses have revealed sparse coding in V1 (e.g. Baddeley et al., 1997; Froudarakis et al., 2014; Haider et al., 2010; Vinje and Gallant, 2000; Weliky et al., 2003; Willmore et al., 2011) that facilitated decoding, maximized coding capacity, and was driven by higher-order statistics of the stimulus. Sensory-evoked activity has been recognized to closely relate to the ongoing spontaneous activity (Berkes et al., 2011; Luczak et al., 2013; Scholvinck et al., 2011; Tsodyks et al., 1999). For example, the structure of spontaneous network dynamics was only modestly altered by naturalistic visual input as determined by similarity in correlation structure of spiking activity (Fiser et al., 2004b). Recently, sparse coding of naturalistic visual input was demonstrated to be state-dependent such that the quiet waking animal employed a less sparse code than the alert animal (Froudarakis et al., 2014). In general, visual responses depend on overall state (Bennett et al., 2013; Niell and Stryker, 2010; Polack et al., 2013). Also, in theoretical models, overall state-defining fluctuations explain response distributions (Goris et al., 2014). Together, these results point towards a model of sensory processing of naturalistic input in which visual responses (1) are sparse and reliable, and (2) emerge from the modulation of ongoing endogenous network dynamics that depend on overall behavioral state. Yet, a limited number of studies have considered the local field potential (LFP) dynamics of naturalistic vision in the awake animal (Brunet et al., 2013; Ito et al., 2011; Kayser et al., 2003; Whittingstall and Logothetis, 2009) and very little is known about the temporal structure of mesoscale network dynamics in V1 across cortical layers measured by the LFP and its relationship to the microscale spiking activity in the awake, freely viewing animal.

Given the recent description of different activity states characterized by the relative presence or absence of slow rhythmic activity in the cortical LFP of awake animals (Harris and Thiele, 2011; Poulet and Petersen, 2008), we here asked (1) how naturalistic visual input modulated the mesoscale V1 activity structure during free viewing in the awake animal, and (2) how the mesoscale activity structure related to the microscopic spiking response. We used the well-known trial-to-trial variability of sensory responses (Tolhurst et al., 1983) as a tool to answer these questions and thereby fill a key gap in our understanding of how sensory input interacts with ongoing network dynamics in the awake animal. In this study, we used the ferret animal model due to its well-studied visual system (Law et al., 1988) and primate-like columnar architecture of V1 (Chapman and Stryker, 1993). We presented full-field nature movie clips to awake, head-fixed ferrets and determined the rhythmic architecture of the LFP before and during visual stimulation (corresponding to spontaneous and sensory-evoked activity) and how these mesoscale network dynamics related to the multiunit spiking response elicited by the visual stimulus as a function of cortical layer.

2. Results

Little is known about the mesoscale network dynamics in V1 of awake animals in absence of experimental constraints such as anesthesia or reward-driven attentional processes that define cortical state by shaping the overall network dynamics. In order to characterize how naturalistic visual input modulates local network activity in the freely-viewing animal, we presented fullfield (58 × 33 degrees visual field) movie clips displaying nature scenes to awake, head-fixed ferrets. The presentation of the movie clips was interleaved with periods of no visual stimulation (spontaneous activity). The visual stimuli exhibited the characteristic 1/f to $1/f^2$ spatial frequency structure of naturalistic stimuli (Figure 1A, left), which is comparable to the spectra of a point-of-view naturalistic visual stimulus (Figure 1A, left middle). Traditionally used synthetic visual stimuli (checkerboard noise pattern, luminance grating) exhibited characteristically different spectra (Figure 1A, right). The animals were acclimated to restraint but did not receive any other behavioral training and the recording sessions did not include any reward contingencies. We verified that the animals were awake during the entirety of the recording sessions by reviewing infrared videography for open eyes and minor movements. Local field potential (LFP) and multiunit activity (MUA) were recorded with multichannel depth probes in V1 (N = 3 animals). Raw LFP traces revealed strikingly different network dynamics for periods of spontaneous activity and visual stimulation (Figure 1B). Prominent high amplitude, low frequency oscillations often occurred during periods of spontaneous network activity; this slow rhythmic activity was typically suppressed for the duration of the visual stimulus. Full-field naturalistic visual input therefore altered overall mesoscale activity in structure in V1, with the most obvious difference present in the low frequencies. Spectral analysis averaged across trials (N = 578) and cortical depth revealed that visual stimulation modulated the power in the entire spectrum included in the analysis (Figure 2A, 0.5 Hz-40 Hz, change in power determined by subtraction of spectra during and before visual stimulation). In particular, power at low frequencies (with the exception of a narrow peak around 6 Hz) was lower during visual stimulation and power at higher frequencies was enhanced with a cross-over frequency of suppression and enhancement around 18 Hz. We mapped this broadband modulation of

oscillatory activity onto the standard frequency bands as determined by the percent of total power for any given frequency band. This provided a measure of the relative presence of oscillations in difference frequency bands (El Boustani et al., 2009). When comparing spontaneous activity (Figure 2B left, median percent ± sem, delta = 31% ± 0.34, theta = 16% ± 0.10, alpha = 13% ± 0.12, beta = 19% ± 0.18, gamma = 21% ± 0.23, n = 578 trials) with visually-driven activity (Figure 2B right, median percent ± sem, delta = 28% ± 0.29, theta = 17% ± 0.11, alpha = 12% ± 0.10, beta = 17% ± 0.12, gamma = 26% ± 0.22, n = 578 trials), delta, alpha, and beta band activity decreased with presentation of visual input and theta and gamma band increased. The mean ranks comparing spontaneous and evoked activity for each of the frequency bands were significantly different (delta: df = 1, H = 29.67, $p<0.0001$; theta: df = 1, H = 10.85, $p=0.001$; alpha: df=1, H = 43.33, $p<0.0001$; beta: df = 1, H = 47.98, $p<0.0001$; gamma: df = 1, H = 190.3, $p<0.0001$; n = 578 trials, Kruskal-Wallis test). Thus, naturalistic visual input caused heterogeneous spectral modulation across all cortical oscillation frequencies, suggesting that naturalistic visual input elicits comprehensive modulation of the overall activity structure in the awake, freely viewing animal presented with full-field naturalistic visual input. Importantly, visual stimulation not only increased fast cortical oscillations but also decreased the presence of slow oscillatory activity both on absolute (Figure 2A) and relative (Figure 2B) scales. To verify that this spectral modulation was not induced by spectral components of the visual stimulus itself, we modeled the spectral properties of responses to the naturalistic videos (Figure 2C). Briefly, we created spatio-temporal receptive fields characteristic of V1, modeled MU responses using these receptive fields as spatial and temporal filters of the visual stimulus, and extracted the frequency information of this MU activity. Indeed, we found that the spectral modulation measured in ferret V1 could not be explained by these modeled responses to the visual stimulus.

We then asked how these changes in mesoscopic network dynamics related to the MUA in response to the visual stimulus. In principle, modulation of mesoscopic LFP activity and microscopic MUA by visual input could reflect two distinct processes. Alternatively, changes in oscillatory activity could define excitability of the local circuitry in V1 and therefore be closely related to the MUA response to the visual input. To disambiguate between these two scenarios, we asked to what extent the trial-to-trial variability of MUA visual responses to the naturalistic visual input was captured by the trial-to-trial variability of the stimulus-induced changes to the oscillation power in the different frequency bands. In one extreme scenario, the trial-to-trial fluctuation in change of LFP power to the visual input would not correlate with the MU trial-to-trial variability, suggesting a decoupling of overall oscillatory tone at the mesoscale and sensory processing at the microscale. Alternatively, changes in LFP power could closely relate to changes in MU responses and therefore be another representation of the same underlying process. In particular, it has long been known that engagement of sensory systems measured by MUA co-occurred with increases in gamma oscillations in the anesthetized animal. We here asked, given the broad spectral modulation that we found at the LFP level in the awake, freely-viewing animal, if and how the classical frequency bands related to the MU response in average across all cortical layers. For each frequency band, we correlated the normalized visual response to the entire stimulus (spike count) with the change in relative LFP power in that given frequency band.

For the delta oscillation, we found a negative correlation, indicating that a stimulus-induced decrease in delta power was associated with a stronger MU responses to the stimulus (Figure 3A, sample LFP and MUA traces; Figure 3B, R = −0.15, 95% CI [−0.23, −0.07], n = 578 trials; correlation coefficient significantly different from 0, $p < 0.001$). In contrast, we found no significant correlation for the theta band (Figure 3C, R = 0.004, 95% CI [−0.078, 0.085], n = 578 trials; correlation coefficient not significantly different from 0, p = 0.93. The alpha oscillation power was also negatively correlated with the MU response, again indicating that the LFP state dynamics were related to the network MU response (Figure 3D, R = −0.24, 95% CI [−0.31, −0.16], n = 578 trials; correlation coefficient significantly different from 0, $p < 0.001$). This correlation coefficient was not statistically different from the corresponding measure for the delta band (Fisher r-to-z transformation, p=0.11). For the beta band, we found a small negative correlation (Figure 3E, R = −0.09, 95% CI [−0.17, −0.008], n = 578 trials; correlation coefficient significantly different from 0, p = 0.03). MU response exhibited a positive correlation with gamma oscillation power (Figure 3F, R = 0.37, 95% CI [0.30, 0.44], n = 578 trials; correlation coefficient significantly different from 0, $p < 0.001$). This correlation coefficient was significantly different from the corresponding measures in the delta (Fisher r-to-z transformation, $p<0.001$) and alpha (Fisher r-to-z transformation, $p<0.001$) frequency bands. Together, these results propose that measurements in LFP power in different frequency bands relate to the MUA such that low frequencies (delta and alpha) correspond to decreased response to visual input whereas increase in the gamma frequency reflects an increased response to the visual stimulus. Importantly, these results suggest that the bidirectional modulation of the oscillatory activity found here directly relates to the microscopic spiking response.

We then asked if the relationship between modulation of oscillation power in individual frequency bands and MUA visual responses exhibited a layer-specific fine-structure. To answer this question, we computed the same correlation coefficients separately for supragranular (LI-LII/III), granular (LIV), and infragranular (LV-VI) layers (Figure 4). Again, the delta, alpha, and gamma bands exhibited the most pronounced correlations with MUA visual responses. The relationship between oscillation recruitment and MUA responses was quite uniform across layers for the alpha (supragranular: R = −0.16, 95% CI [−0.26 −0.061]; granular: R = − 0.18, 95% CI [−0.26 −0.96]; infragranular: R= −0.14, 95% CI [−0.22 −0.054]) and gamma (supragranular: R = 0.29, 95% CI [0.19 0.38]; granular: R = 0.31, 95% CI [0.23 0.39]; infragranular: R= 0.30, 95% CI [0.23 0.38]) frequency bands. However, several interesting additional features became apparent in this analysis. First, the negative correlation between recruitment of delta oscillation and MUA response was absent for supragranular layers (R = −0.073, 95% CI: [−0.18 0.031]) but not for granular (R = −0.20, 95% CI: [−0.28 −0.11]) and infragranular (R = −0.16, 95% CI: [−0.24 −0.076]) layers. Theta oscillation recruitment weakly correlated with MUA responses exclusively in the granular layer (R = 0.086, 95% CI [0.0019 0.17]; supragranular: R = 0.02, 95% CI [−0.084 0.12]; infragranular: R = 0.0047, 95% CI [−0.087 0.078]). Beta oscillation recruitment was negatively correlated with MUA responses only in the supragranular layers (R = −0.12, 95% CI [−0.22 −0.017]; granular: R = −0.062, 95% CI [−0.15 .022]; infragranular: R = 0.026, 95% CI [−0.057 0.11]). This layer-specific fine structure may reflect local differences in the functional role of oscillatory activity within the V1

microcircuit or the preferential target layers of incoming connections that use specific oscillation frequencies as their signal. Thus, these data suggest the presence of an endogenous trade-off between slow (delta and alpha) and fast (gamma) oscillation power that is modulated by visual input and shapes the spiking response to naturalistic visual input.

In addition to the relationship between time-averaged MUA and oscillatory power, MUA has been shown to exhibit preferred phase-of-firing according to the ongoing oscillation in different frequencies (Masquelier et al., 2009). Therefore, we next asked if MUA exhibited a preferred phase-of-firing, and if these faster timescale dynamics were also modulated by presentation of naturalistic visual stimuli. We found that MUA exhibited the strongest preferred phase-of-firing for the delta oscillation both during spontaneous activity and visual stimulation (Figure 5A, example high-pass filtered trace and delta-frequency band-pass filtered LFP trace. Figure 5B and 5C, left: preferred phase of firing for delta oscillation = −2.83 radians). Kullback-Leibler (KL) divergence was calculated as a metric of non-uniformity of MUA phase distribution (Figure 5D, median KL divergence and 95% CI: spontaneous activity, delta = 0.0068 [0.0066 0.0070]; visual stimulation, delta = 0.0023 [0.0022 0.0024]). Naturalistic visual stimulation decreased the strength of preference for phase-of-firing, particularly in the lower frequencies (Figure 5D, median KL divergence during spontaneous activity and 95 % CI: theta = 0.0037 [0.0035 0.0038], alpha = 0.0018 [0.0017 0.0019], beta = 0.0005 [0.0004 0.0005], gamma = 0.0002 [0.0002 0.0002], median KL divergence during visual stimulation and 95% CI: theta = 0.0008 [0.0007 0.0009], alpha = 0.0005 [0.0005 0.0006], beta = 0.0004 [0.0003 0.0004], gamma = 0.0002 [0.0002 0.0002]). Therefore, naturalistic visual input weakened the strength of coupling between MUA and phase of the ongoing oscillation. Together, these data suggest that the low frequency oscillations are not only decreased in amplitude but also had less influence on spike-timing during presentation of naturalistic visual input.

We next investigated the time-course of the modulation of the LFP spectrum, in particular of the delta, alpha, and gamma bands that we found to be correlated with the MUA response. In order to gain resolution in the time-domain, we used the Hilbert transformation to extract the time-course of the power in the different frequency bands for LFP activity in three groups of cortical layers (supragranular: LI-LII/III, granular: LIV, and infragranular: LV-VI). We used a two-dimensional state-space representation defined by delta and gamma power (averaged across trials) to characterize the dynamics of the band-limited oscillation power. Trajectories in state space that separate into two clusters, connected by transients at stimulation onset and offset, would indicate that presentation of naturalistic visual input switched the V1 network between two states. Alternatively, lack of separation of the epochs corresponding to spontaneous activity and visual stimulation would support a model in which relative oscillation strength in different frequencies occurs on a continuum without clear separation into distinct network states. In agreement with the former model of distinct states, the delta-gamma phase plots demonstrated clear clustering into two relatively distinct states with transitions at stimulus onset and offset for all three groups of cortical layers (Figure 6). At stimulation onset, an initially transient (light blue) characterized by an increase in both gamma and delta power was followed by a state switch that corresponded to a reduction of delta power and a concomitant increase of gamma power. Importantly, the transients between the two states were quite pronounced and lasted up to several seconds, in particular

at the offset of the stimulus (orange time points). Although the offset transient quickly moved the trajectory back to the state corresponding to spontaneous activity (marked as “I” in Figure 6C), an extra “rebound detour” occurred before final convergence (marked as “II”), in particular for deep layers. Similarly, for the state space representation of the alpha-gamma power pair, we again found two distinct clusters (Figure 7). Stimulus onset induced a switch from a high alpha, low gamma power state to a low alpha, high gamma power state. Interestingly, the offset transient lasted several seconds and mostly corresponded to a recovery of the spontaneous alpha oscillation levels (near horizontal orange part of the trajectories). Together, this state-space analysis proposes that free viewing of naturalistic stimuli induced a state transition from a cortical state characterized by relative dominance of delta and alpha oscillations to a cortical state characterized by the relative dominance of the gamma oscillation. To test this model, we used k-means clustering to assay for the presence of two distinct clusters and measured the number of misclassification as an indicator for poorly captured structure by two clusters. Mostly, the two clusters determined by k-means clustering indeed corresponded to spontaneous and evoked activity. We quantified the percent of data points which were incorrectly clustered for each group of cortical layers. For both delta-gamma and alpha-gamma trajectories, supragranular layers exhibited less accurate clustering, with significantly more incorrectly clustered data points than granular or infragranular layers (Figure 8, percent incorrectly clustered ± sem for supragranular, granular, and infragranular respectively; bars represent medians across 100 iterations of bootstrapping. Delta-gamma: 6.78% ± 0.24, 0.69% ± 0.07, 1.03% ± 0.08; Alpha-gamma: 6.42% ± 0.25, 2.28% ± 0.15, 3.48% ± 0.12, comparisons significant at $p < 0.05$ are noted). These results further support the presence of two distinct states that are governed by the same trade-off of delta and alpha versus gamma band activity. Transitions for gamma oscillation power were relatively fast but the delta and alpha oscillation power transients lasted up to several seconds, suggesting a slow transition between the two states.

The distinct states described above were described by the relative power between slow and fast frequency oscillations. Substantial work has demonstrated the importance of coordination between the phase of low frequencies and amplitude of higher frequency oscillations (Canolty and Knight, 2010). Thus, we asked whether the two distinct states defined by delta or alpha power vs gamma power also exhibited differences in the phase-amplitude coupling (PAC) of slow and fast frequencies. Indeed, we found that both delta-gamma and alpha-gamma PAC were lower during the state elicited by presentation of naturalistic visual stimuli compared to spontaneous activity (Figure 9). Interestingly delta-gamma PAC differed less between the two states, particularly in the granular layer (Figure 9B, right). In other words, alpha-gamma PAC was more strongly modulated by visual stimulation. This result is in agreement with our finding that alpha power is more highly correlated with MU spiking activity, compared to delta power. Together, these results demonstrate that the state change induced by visual stimulation is characterized by a change in the balance between low and high frequencies and also by a decoupling of slow and fast oscillations.

3. Discussion

Our understanding of the visual system is mostly based on the neuronal responses to synthetic, optimized stimuli presented to anesthetized animals. Recent work that employed naturalistic visual input provided a new perspective on visual coding and the modulatory rather than driving nature of sensory input both in animal models (Belitski et al., 2008; Besserve et al., 2010; Dan et al., 1996; David et al., 2004; Fiser et al., 2004a; Gallant et al., 1998; Ito et al., 2011; MacEvoy et al., 2008; Mazzoni et al., 2008; Mazzoni et al., 2011a; Mazzoni et al., 2011b; Montemurro et al., 2008; Reinagel, 2001; Smyth et al., 2003a; Vinje and Gallant, 2000; Wang et al., 2007; Weliky et al., 2003; Whittingstall and Logothetis, 2009) and in human imaging studies (e.g. Betti et al., 2013). However, surprisingly little is known about network dynamics in absence of experimentally induced constraints such as anesthesia, which selectively increase delta oscillations and suppress alpha oscillation in visual cortex (Purdon et al., 2013), or attention paradigms that use reward-based approaches that selectively modulate gamma oscillations as a function of the specific attentional demands (Buschman and Miller, 2007). We here sought to fill in this gap of knowledge about the mesoscale network dynamics in V1 during free viewing of naturalistic visual input.

We found that free viewing of naturalistic visual stimuli (movie clips of nature scenes) modulated cortical oscillations in all frequency bands; most prominently, the delta and alpha frequency bands were suppressed and the gamma frequency band was enhanced. Analysis of the time-course of the instantaneous power in these frequency bands demonstrated that visual stimuli switched the overall network between two distinct states at the onset and offset of the stimulus, respectively. These LFP dynamics were related to the microscopic MUA responses to the visual stimuli. Both the delta and alpha frequency bands negatively correlated with the MU responses and explained a moderate amount of the trial-to-trial variability of the MU response. Stimulus-elicited changes in the gamma frequency band positively correlated with the MU response. Together, these data propose that V1 switches between distinct states that are defined by the relative presence of delta and alpha oscillations on the one hand side and gamma oscillations on the other hand side.

Our data agree with previous studies that consistently found gamma oscillations to be a marker of visual processing for a large number of different visual stimuli and experimental conditions. Most importantly in the context of our results, naturalistic visual input increased gamma oscillations in awake primates (Brunet et al., 2013; Ito et al., 2011; Whittingstall and Logothetis, 2009) and cats (Kayser et al., 2003). Similar to our results, recruitment of gamma oscillations correlated with MU responses in the awake, fixating primate (Whittingstall and Logothetis, 2009). Gamma oscillations arise from local circuit interactions, specifically from the dynamic interaction of principle cells and parvalbumin-positive, fast-spiking inhibitory interneurons (Cardin et al., 2009; Sohal et al., 2009). Likely, excitatory afferent drive caused by the visual stimulation increased spiking activity in V1 and concomitantly the power in the gamma band. In contrast to our results, previous studies (e.g. Belitski et al., 2008) reported a stimulus-induced increase in the low frequencies (but see: Kayser et al., 2003) and found a positive correlation between low frequency activity and spiking response (Whittingstall and Logothetis, 2009). These differences may be explained

by the fact that our paradigm did not include application of anesthetics or behavioral contingencies that would have shaped the behavioral state of the animal and might have suppressed the state transitions with visual stimulation as found in our study.

At the macroscopic level of human electroencephalograms (EEGs), both alpha and delta oscillations have emerged as regulators of overall network excitability. Specifically, human studies have consistently found that the power and phase of the alpha oscillation measured with EEG or MEG modulated threshold sensory responses (Busch et al., 2009; Ergenoglu et al., 2004; Hanslmayr et al., 2007; Palva and Palva, 2007; van Dijk et al., 2008). Our results of stronger visual responses on trials with more stimulus-induced suppression of the delta and alpha frequency band conceptually agree with the functional role of these macroscopic network dynamics. Importantly, however, we did not employ threshold sensory stimuli nor did we require specific behavioral responses. Rather, we used naturalistic full-field visual input without any experimental contingencies. Our results therefore propose that (1) the functional roles of these mesoscale oscillations relate to the macroscopic dynamics in human EEG studies and (2) that the regulation of MUA in V1 reflects the underlying mechanism of differential responses as a function of delta and alpha oscillations measured by EEG.

Sensory responses not only reflect the properties of the physical input but also the state of the sensory system before and during the receipt of incoming information. Separation of endogenous state dynamics of neuronal networks and sensory responses is fundamentally difficult to achieve since any input – at least in theory - perturbs the state of the system. To mitigate this confound, studies of state-dependent sensory processing typically employ brief, weak stimuli (Castro-Alamancos, 2004; Curto et al., 2009; Haider et al., 2007; Hasenstaub et al., 2007; Worgotter et al., 1998) and implicitly assume that the stimulus itself does not change global brain state. These studies demonstrated the role of oscillatory activity in regulating excitability and therefore sensory responses. In contrast, our study provides a different perspective in which the sensory stimulus itself (10 sec of full-field naturalistic visual input) switches overall cortical state. Such state transitions between slow rhythmic and desynchronized states have been recently reported to spontaneously occur in both the somatosensory and the auditory system of rodents (Luczak et al., 2013; Poulet and Petersen, 2008). Our study shows a similar presence of slow rhythmic activity in the awake, resting ferret. Of note, not all recent work in awake animals found such rhythmic structure. These differences may be due to different experimental conditions where for example, animals received intermittent rewards during head fixation (Haider et al., 2013) and therefore assumed an anticipatory behavioral state, or where animals exhibited heightened, experimentally-induced noradrenergic tone (Constantinople and Bruno, 2011). Together, our findings support the existence of a state characterized by the relative dominance of delta and alpha oscillations and a state characterized by the relative dominance of the gamma oscillation (as identified by the trial-averaged phase-space representation and the subsequent k-means clustering).

As a notable limitation, our study did not probe the underlying mechanism for the meso- and microscale dynamics described here. Likely candidate mechanisms are modulation of neuromodulatory tone, top-down modulation by higher-order cortical areas such as prefrontal cortex, and state switching in thalamo-cortical loops due to increased

depolarization by the afferent visual input from the retina to the thalamus. Each of these mechanisms may individually or together contribute to the dynamics described here. Changes in cholinergic tone are associated with changes in attentional state (Harris and Thiele, 2011; Lee and Dan, 2012); increased cholinergic tone has broad effects on intrinsic and synaptic properties, with the main effect at the meso- and macroscale being a desynchronization that typically corresponds to a selective suppression of low frequency network activity (Metherate et al., 1992). Stimulation of brainstem cholinergic centers leads to tonic depolarization of cortical neurons (Steriade et al., 1993a; Steriade et al., 1993b), and stimulation of cortical sources of cholinergic innervation produces awake-like cortical activity in anesthetized animals (Goard and Dan, 2009; Metherate et al., 1992; Steriade et al., 1993a; Steriade et al., 1993b). Release of neocortical acetylcholine shifted subthreshold membrane potential fluctuations from slow, delta oscillations to low-amplitude, gamma frequency oscillation (Metherate et al., 1992). Although no experimental contingency provided an incentive for the animals in our study to pay attention to the visual stimulus, the onset of the visual stimuli in absence of other salient sensory input may still have recruited cholinergic modulation by means of sensory-driven, bottom-up attention. Top-down modulation from higher order cortical areas could also provide (possible concomitantly or synergistically with changes in neuromodulatory tone) different network set-points as recently described in the somatosensory system (Zagha et al., 2013). Third and last, cortical activity arises from the thalamocortical interaction in the canonical circuit that consists of the primary thalamic nucleus (in case of the visual system the lateral geniculate nucleus, LGN), the primary cortical target, here V1, and the reticular nucleus. Thalamo-cortical relay cells exhibit bistable behavior in which, as a result of depolarization and overall neuromodulatory tone, neurons either exhibit burst firing that facilitates slow rhythmic activity in the thalamo-cortical loop or tonic spiking that corresponds to an “activated” or desynchronized cortex (Steriade et al., 1993b). In this scenario, afferent sensory input would provide the necessary drive to induce such transitions between the two states. Related to this, it remains to be studied if the network dynamics described here are unique to V1, or if these properties are more ubiquitous throughout cortical regions. Specific parameters which may affect the network dynamics described here may include cell populations, innervation by other brain regions, and feedback within a given brain region and with other brain regions (e.g. thalamocortical loops).

Together, our work provides a novel perspective on the mesoscale network dynamics in V1 of the awake, freely viewing animal. We found that naturalistic visual input switched cortical state in the freely viewing animal and that the balance between delta and alpha oscillations on the one hand side and gamma oscillations on the other hand side may provide a mechanism by which sensory responsiveness is adjusted on a trial-to-trial basis. Our work therefore proposes that using more naturalistic experimental approaches to visual stimulation offers an important, complementary perspective on how mesoscopic state dynamics mediate sensory processing. Eventually, such insights could provide a network-level understanding of sensory processing deficits in patients with schizophrenia and autism, disease state that have been recently associated deficits in cortical oscillatory activity (Uhlhaas and Singer, 2012).

4. Experimental Procedures

4.1 Acclimation and Surgery

Female ferrets (*Mustela putoris furo*, supplied by Marshall BioResources, 15–20 weeks old at study onset, 750–1000g, n = 3) were used in this study. Surgical and electrophysiological recording procedures were described in detail previously (Sellers et al., 2013). The growth of female ferrets plateaus prior to the age used here, making females more suited than males for chronic chamber implants. All animals were spayed by the vendor in case they were kept past the age of sexual maturity; in this study, all animals were used prior to the age of sexual maturity. Animals were acclimated to be calmly restrained for up to two hours. Subsequently, animals underwent aseptic surgery in preparation for electrophysiological recordings in primary visual cortex (V1). An initial intramuscular injection of ketamine (30 mg/kg) and xylazine (1–2 mg/kg) was used for anesthesia induction. Deep anesthesia was maintained for the duration of the surgery with supplemental intramuscular injections of ketamine and xylazine, approximately every 40 minutes. This anesthesia paradigm was designed to achieve general anesthesia throughout surgery, and was assayed by complete absence of withdrawal response to toe pinch. Physiologic monitors included electrocardiogram, pulse oxygen level, and rectal body temperature. Animals were warmed with a water heating blanket to maintain rectal body temperature of 38.0–39.0°C. The animal's eyes were protected with paralube for the duration of surgery.

Surgical procedures consisted of an initial midline incision of the scalp, retraction of the soft tissue, and a circular craniotomy located over V1 (approximately 3 mm anterior to lambda and 9 mm lateral to the midline). The potential for swelling was reduced with an injection of furosemide (1mg/kg, IM). After removal of dura, the brain was covered with warm sterile 4% agar. A custom-fabricated cylindrical chamber with a removable cap (material: Ultem 1000) was cemented to the skull in order to allow subsequent access to the craniotomy for recordings. Additionally, a stainless steel head post was implanted with bone screws and dental cement. Upon completion of these surgical procedures, the incision was closed with sutures and treated with antibiotic cream. Yohimbine (0.25–0.5mg/kg, IM) was administered to reverse anesthesia. The animal was kept warm with a heating blanket and observed during recovery from anesthesia. Meloxicam (0.2mg/kg, IM) and enrofloxacin (5mg/kg, IM) were administered to prevent infection and to minimize post-surgical discomfort for five days post-surgery. Animals were allowed to fully recover from surgery (at least 7 days) before the first recording session. All procedures were approved by the UNC- Chapel Hill IACUC and exceed guidelines set forth by the NIH and USDA.

4.2 Multichannel Extracellular Recordings

Local field potential (LFP) and multiunit activity (MUA) were recorded during spontaneous activity and presentation of naturalistic visual stimuli. During each recording session, animals were restrained, head-fixed, and the recording chamber was opened. After rinsing the craniotomy site with sterile saline, a linear 32-channel depth probe (Neuronexus, Ann Arbor, MI) was acutely inserted perpendicular to the surface of cortex to record from all cortical layers simultaneously. Recording sites were spaced 50μm apart along the z-axis, with the reference electrode located on the same shank (0.5mm above the top recording

site). Probes were slowly advanced into cortex using a micromanipulator (Narishige, Tokyo, Japan), and correct depth placement was determined by small amplitude deflections of the LFP at superficial electrode sites and large amplitude deflections of the LFP at deeper electrode sites. Current source density (CSD) analysis was conducted offline to determine location of recording electrode relative to cortical layer IV (see Data Analysis). All electrode penetrations were made within 1mm of the same location in V1, corresponding to 5 degrees visual field in azimuth and 4.8 degrees visual field in elevation (given magnification factors in area 17 of 0.2mm in cortex/degrees of visual space in the azimuth, and 0.207mm in cortex/degrees of visual space in elevation) (Cantone et al., 2005).

Raw signals were first amplified with MPA8I head-stages with gain 10 (Multichannel Systems, Reutlingen, Germany) and then further amplified with gain 500, (Model 3500, A-M Systems, Carlsborg, WA), digitized at 20 kHz (Power 1401, Cambridge Electronic Design, Cambridge, UK), and digitally stored using Spike2 software (Cambridge Electronic Design). All recordings were conducted with room lights off and with minimal acoustic noise to prevent contamination of the recording with neuronal responses to extraneous stimuli.

Upon correct depth placement of the electrode, the animal was presented with naturalistic visual stimuli (four different movie clips from Planet Earth, BBC, London, UK) on a 52 × 29 cm monitor with 120Hz refresh rate and full high definition resolution (1,920 × 1,080 pixels, GD235HZ, Acer Inc., New Taipei City, Taiwan) at 47cm distance from the animal. Visual stimuli filled 58 degrees of the visual field horizontally, 33 degrees of the visual field vertically, and was controlled by the Psychophysics toolbox (Brainard, 1997) for MATLAB and a GeForce580 GPU (NVIDIA, Santa Clara, CA). Correct timing of individual display frames was ascertained by a photodiode covering a small flashing square in the corner of the monitor. Each trial of visual stimulation contained 10 seconds of dark control before visual stimulation (to record spontaneous activity), 10 seconds of Planet Earth footage (movie of animals moving across the screen), and 10 seconds dark control after visual stimulation. For a few sessions, only a subset of stimuli was used to shorten the duration of the head-restraint. Continuous video recording with an infrared sensitive camera (Handycam HDR-cx560v, Sony, Tokyo, Japan) and LED infrared illumination was used to document that the animal was fully awake during recordings as evidenced by whisking and noise twitching. At the conclusion of the study, all animals were humanely killed with an overdose of sodium pentobarbital and immediately perfused with 4% formaldehyde in 0.1M phosphate buffered saline for subsequent histological verification of recording locations.

4.3 Data Analysis

Recorded signals were processed offline with custom-written scripts in MATLAB (Mathworks, Natick, MA). Current source density (CSD) was calculated in order to determine the location of the 32-channel probes relative to cortical layers. Cortical layers were aligned across different electrode penetrations according to putative granular layer IV. CSD was determined by calculating the second spatial derivative of the low-pass filtered and smoothed LFP in response to full-field flashes (white screen) of duration 32ms, presented at a rate of 1Hz. The first stimulus-evoked sink in the laminar profile is indicative of layer IV

(Mitzdorf, 1985). As additional verification of probe placement, MU firing rate was calculated for 30–50ms post stimulus onset. A subset of trials was manually excluded due to motion artifacts in the LFP signal, determined by extreme values in the raw traces. In order to calculate the spatial frequency of the visual stimuli, the video was converted to gray scale and a two-dimensional discrete Fourier transform was calculated on a square region of each frame. Rotational averaging was used to reduce the two dimensional power spectrum to one dimension. The same procedure was conducted to calculate spatial frequency of a stock image of a naturalistic visual stimulus (from the point-of-view of an animal) and for two artificial visual stimuli (black and white checkerboard noise and luminance gratings). Data from different naturalistic visual stimulus movies were pooled (n = 578 trials). Data are presented per trial, averaged across electrodes, unless otherwise noted. Values are reported as median ± sem (standard error of the mean). The spectral content of the LFP was determined by convolving the raw extracellular voltage signals with a family of Morlet wavelets (0.5Hz – 40Hz, step-width 0.5Hz) with normalized amplitude, providing an optimal trade-off between time and frequency uncertainty (Goupillaud et al., 1984). Power in each frequency band (delta = 0.5–4Hz, theta = 4–8Hz, alpha = 8–12Hz, beta = 12–20Hz, gamma = 20–40Hz) was calculated for each trial. Relative power was determined by calculating the percent of total power in each frequency band, on a trial-by-trial basis. Relative power enhancement was calculated by dividing the relative power during visual stimulation by the relative power during spontaneous activity before stimulation, on a trial-by-trial basis. We wanted to test if observed spectral modulation of the LFP was induced by spectral properties of the visual stimulus. To do so, we employed a linear-nonlinear model of V1 spatio-temporal receptive fields and used these as spatial and temporal filters of the 10 second movie clips (Mante et al., 2008; Ringach, 2004). Modeled MU activity was peak-normalized, and the spectrum was calculated using the fast Fourier transform. MU action potential firing was detected by high-pass filtering the data (4th order Butterworth filter, 300Hz cutoff) and imposing a threshold of −3*std. MU firing rate enhancement was calculated by dividing MU firing rate during visual stimulation by MU firing rate during spontaneous activity before stimulation, on a trial-by-trial basis. Correlation coefficients were calculated using MATLAB function corrcoef, and significance was calculated by using the Fisher r-to-z transformation.

To determine the preferred phase-of-firing of MUA for each frequency band, the instantaneous phase was calculated using the Hilbert transform on band-pass filtered data (delta = 0.5–4Hz, theta = 4–8Hz, alpha = 8–12Hz, beta = 12–20Hz, gamma = 20–40Hz). Peak phase-of-firing was determined as the phase with the highest probability of spiking. Kullback-Leibler (KL) divergence was used to determine the difference of the resulting preferred phase-of-firing histograms from a flat distribution. To determine the time-course of the band-limited power in the five frequency bands, we used the Hilbert transform on band-pass filtered data (delta = 0.5–4Hz, theta = 4–8Hz, alpha = 8–12Hz, beta = 12–20Hz, gamma = 20–40Hz) to determine the instantaneous amplitude in each frequency band. This allowed for trajectory plots of the oscillatory activity in frequency-band pairs of interest (phase space plots of instantaneous amplitudes in frequency bands of interest). We conducted k-means clustering of normalized amplitudes (at all time-steps) in order to quantify if behavioral states could be differentiated based on oscillatory activity. We

requested clustering into two clusters based on visual inspection of the phase-space plots. We did not include the one second of data immediately following onset and offset of the stimulus in k-means clustering, as we were interested in the equilibrium states corresponding to spontaneous activity and visual stimulation rather than transients at stimulation onset and offset. Correctly clustered refers to trials which were categorized correctly based on if the data originated from a spontaneous activity or visually-evoked data point. Phase-amplitude coupling was calculated between the phase of low frequencies (delta or alpha) and the amplitude of the gamma oscillation, according to (Voytek et al., 2010). Briefly, the raw signal was band pass filtered at the low frequency of interest (delta or alpha) and the gamma frequency. The amplitude of the gamma-filtered signal was extracted, and then filtered at the lower frequency of interest. The phase of both signals was extracted and phase-amplitude coupling was calculated as the mean vector between the angles.

Bootstrapping with 100 iterations of resampling with replacement, a distribution-independent method, was used to calculate standard errors when parametric models were inappropriate. The non-parametric Kruskall-Wallis test was used to determine statistical significance (if the samples of interest came from the same distribution) and multiple comparisons were corrected for using Tukey's honestly significant difference criterion.

Acknowledgments

The authors thank the members of the Frohlich Lab for support, particularly Stephanie Belhorn for help with handling of the animals.

Grants: This work was supported by UNC Psychiatry, UNC School of Medicine, and the Foundation of Hope. Research reported in this publication was partially supported by the National Institute of Mental Health of the National Institutes of Health under Award Number R01MH101547. The content is solely the responsibility of the authors and does not necessarily represent the official views of the National Institutes of Health.

References

Baddeley R, et al. Responses of neurons in primary and inferior temporal visual cortices to natural scenes. Proceedings of the Royal Society of London. Series B: Biological Sciences. 1997; 264:1775–1783.

Barlow, H. Possible principles underlying the transformations of sensory messages. In: Rosenblith, W., editor. Sensory Communication. MIT Press; 1961. p. 217-234.

Belitski A, et al. Low-frequency local field potentials and spikes in primary visual cortex convey independent visual information. The Journal of neuroscience : the official journal of the Society for Neuroscience. 2008; 28:5696–709. [PubMed: 18509031]

Bennett C, Arroyo S, Hestrin S. Subthreshold mechanisms underlying state-dependent modulation of visual responses. Neuron. 2013; 80:350–7. [PubMed: 24139040]

Berkes P, et al. Spontaneous cortical activity reveals hallmarks of an optimal internal model of the environment. Science. 2011; 331:83–7. [PubMed: 21212356]

Besserve M, et al. Causal relationships between frequency bands of extracellular signals in visual cortex revealed by an information theoretic analysis. Journal of computational neuroscience. 2010; 29:547–66. [PubMed: 20396940]

Betti V, et al. Natural scenes viewing alters the dynamics of functional connectivity in the human brain. Neuron. 2013; 79:782–797. [PubMed: 23891400]

Brainard DH. The Psychophysics Toolbox. Spatial vision. 1997; 10:433–6. [PubMed: 9176952]

Brunet N, et al. Visual Cortical Gamma-Band Activity During Free Viewing of Natural Images. Cerebral cortex. 2013

Busch NA, Dubois J, VanRullen R. The phase of ongoing EEG oscillations predicts visual perception. The Journal of neuroscience : the official journal of the Society for Neuroscience. 2009; 29:7869–76. [PubMed: 19535598]

Buschman TJ, Miller EK. Top-down versus bottom-up control of attention in the prefrontal and posterior parietal cortices. Science. 2007; 315:1860–2. [PubMed: 17395832]

Canolty RT, Knight RT. The functional role of cross-frequency coupling. Trends Cogn Sci. 2010; 14:506–15. [PubMed: 20932795]

Cantone G, et al. Feedback connections to ferret striate cortex: direct evidence for visuotopic convergence of feedback inputs. The Journal of comparative neurology. 2005; 487:312–31. [PubMed: 15892103]

Cardin JA, et al. Driving fast-spiking cells induces gamma rhythm and controls sensory responses. Nature. 2009; 459:663–7. [PubMed: 19396156]

Castro-Alamancos MA. Absence of rapid sensory adaptation in neocortex during information processing states. Neuron. 2004; 41:455–64. [PubMed: 14766183]

Chapman B, Stryker MP. Development of orientation selectivity in ferret visual cortex and effects of deprivation. The Journal of neuroscience : the official journal of the Society for Neuroscience. 1993; 13:5251–62. [PubMed: 8254372]

Constantinople CM, Bruno RM. Effects and mechanisms of wakefulness on local cortical networks. Neuron. 2011; 69:1061–8. [PubMed: 21435553]

Curto C, et al. A simple model of cortical dynamics explains variability and state dependence of sensory responses in urethane-anesthetized auditory cortex. The Journal of neuroscience : the official journal of the Society for Neuroscience. 2009; 29:10600–12. [PubMed: 19710313]

Dan Y, Atick JJ, Reid RC. Efficient coding of natural scenes in the lateral geniculate nucleus: experimental test of a computational theory. The Journal of neuroscience: the official journal of the Society for Neuroscience. 1996; 16:3351–3362. [PubMed: 8627371]

David SV, Vinje WE, Gallant JL. Natural Stimulus Statistics Alter the Receptive Field Structure of V1 Neurons. The Journal of Neuroscience. 2004; 24:6991–7006. [PubMed: 15295035]

El Boustani S, et al. Network-state modulation of power-law frequency-scaling in visual cortical neurons. PLoS Comput Biol. 2009; 5:e1000519. [PubMed: 19779556]

Ergenoglu T, et al. Alpha rhythm of the EEG modulates visual detection performance in humans. Brain research. Cognitive brain research. 2004; 20:376–83. [PubMed: 15268915]

Felsen G, Dan Y. A natural approach to studying vision. Nature neuroscience. 2005; 8:1643–6.

Fiser J, Chiu C, Weliky M. Small modulation of ongoing cortical dynamics by sensory input during natural vision. Nature. 2004a; 431:573–578. [PubMed: 15457262]

Fiser J, Chiu CY, Weliky M. Small modulation of ongoing cortical dynamics by sensory input during natural vision. Nature. 2004b; 431:573–578. [PubMed: 15457262]

Froudarakis E, et al. Population code in mouse V1 facilitates readout of natural scenes through increased sparseness. Nature neuroscience. 2014; 17:851–7.

Gallant JL, Connor CE, Van Essen DC. Neural activity in areas V1, V2 and V4 during free viewing of natural scenes compared to controlled viewing. NeuroReport. 1998; 9:2153–2158. [PubMed: 9674611]

Goard M, Dan Y. Basal forebrain activation enhances cortical coding of natural scenes. Nat Neurosci. 2009; 12:1444–9. [PubMed: 19801988]

Goris RLT, Movshon JA, Simoncelli EP. Partitioning neuronal variability. Nature Neuroscience. 2014; 17:858–865.

Goupillaud P, Grossmann A, Morlet J. Cycle-Octave and Related Transforms in Seismic Signal Analysis. Geoexploration. 1984; 23:85–102.

Haider B, et al. Enhancement of visual responsiveness by spontaneous local network activity in vivo. Journal of neurophysiology. 2007; 97:4186–202. [PubMed: 17409168]

Haider B, et al. Synaptic and network mechanisms of sparse and reliable visual cortical activity during nonclassical receptive field stimulation. Neuron. 2010; 65:107–21. [PubMed: 20152117]

Haider B, Hausser M, Carandini M. Inhibition dominates sensory responses in the awake cortex. Nature. 2013; 493:97–100. [PubMed: 23172139]

Hanslmayr S, et al. Prestimulus oscillations predict visual perception performance between and within subjects. NeuroImage. 2007; 37:1465–73. [PubMed: 17706433]

Harris KD, Thiele A. Cortical state and attention. Nature reviews. Neuroscience. 2011; 12:509–23.

Hasenstaub A, Sachdev RN, McCormick DA. State changes rapidly modulate cortical neuronal responsiveness. The Journal of neuroscience : the official journal of the Society for Neuroscience. 2007; 27:9607–22. [PubMed: 17804621]

Hubel DH, Wiesel TN. Receptive fields of single neurones in the cat's striate cortex. The Journal of Physiology. 1959; 148:574–591. [PubMed: 14403679]

Ito J, et al. Saccade-Related Modulations of Neuronal Excitability Support Synchrony of Visually Elicited Spikes. Cerebral Cortex. 2011; 21:2482–2497. [PubMed: 21459839]

Kayser C, Salazar RF, Konig P. Responses to natural scenes in cat V1. Journal of neurophysiology. 2003; 90:1910–1920. [PubMed: 12750423]

Law MI, Zahs KR, Stryker MP. Organization of primary visual cortex (area 17) in the ferret. The Journal of comparative neurology. 1988; 278:157–80. [PubMed: 3068264]

Lee SH, Dan Y. Neuromodulation of brain states. Neuron. 2012; 76:209–22. [PubMed: 23040816]

Luczak A, Bartho P, Harris KD. Gating of sensory input by spontaneous cortical activity. J Neurosci. 2013; 33:1684–95. [PubMed: 23345241]

MacEvoy SP, Hanks TD, Paradiso MA. Macaque V1 Activity During Natural Vision: Effects of Natural Scenes and Saccades. Journal of Neurophysiology. 2008; 99:460–472. [PubMed: 18077668]

Mante V, Bonin V, Carandini M. Functional mechanisms shaping lateral geniculate responses to artificial and natural stimuli. Neuron. 2008; 58:625–38. [PubMed: 18498742]

Masquelier T, et al. Oscillations, phase-of-firing coding, and spike timing-dependent plasticity: an efficient learning scheme. J Neurosci. 2009; 29:13484–93. [PubMed: 19864561]

Mazzoni A, et al. Encoding of naturalistic stimuli by local field potential spectra in networks of excitatory and inhibitory neurons. PLoS computational biology. 2008; 4:e1000239–e1000239. [PubMed: 19079571]

Mazzoni A, et al. Cortical dynamics during naturalistic sensory stimulations: experiments and models. Journal of physiology, Paris. 2011a; 105:2–15.

Mazzoni A, et al. Cortical dynamics during naturalistic sensory stimulations: experiments and models. Journal of physiology, Paris. 2011b; 105:2–15.

Metherate R, Cox CL, Ashe JH. Cellular bases of neocortical activation: modulation of neural oscillations by the nucleus basalis and endogenous acetylcholine. The Journal of neuroscience : the official journal of the Society for Neuroscience. 1992; 12:4701–11. [PubMed: 1361197]

Mitzdorf U. Current source-density method and application in cat cerebral cortex: investigation of evoked potentials and EEG phenomena. Physiological reviews. 1985; 65:37–100. [PubMed: 3880898]

Montemurro, Ma, et al. Phase-of-firing coding of natural visual stimuli in primary visual cortex. Current biology : CB. 2008; 18:375–80. [PubMed: 18328702]

Niell CM, Stryker MP. Modulation of visual responses by behavioral state in mouse visual cortex. Neuron. 2010; 65:472–9. [PubMed: 20188652]

Olshausen BA, Field DJ. How close are we to understanding v1? Neural computation. 2005; 17:1665–99. [PubMed: 15969914]

Palva S, Palva JM. New vistas for α-frequency band oscillations. Trends in neurosciences. 2007; 30:150–158. [PubMed: 17307258]

Polack PO, Friedman J, Golshani P. Cellular mechanisms of brain state-dependent gain modulation in visual cortex. Nature neuroscience. 2013; 16:1331–9.

Poulet JF, Petersen CC. Internal brain state regulates membrane potential synchrony in barrel cortex of behaving mice. Nature. 2008; 454:881–5. [PubMed: 18633351]

Purdon PL, et al. Electroencephalogram signatures of loss and recovery of consciousness from propofol. Proceedings of the National Academy of Sciences of the United States of America. 2013; 110:E1142–51. [PubMed: 23487781]

Reinagel P. How do visual neurons respond in the real world? Current Opinion in Neurobiology. 2001; 11:437–442. [PubMed: 11502389]

Ringach DL. Mapping receptive fields in primary visual cortex. J Physiol. 2004; 558:717–28. [PubMed: 15155794]

Ruderman DL, Bialek W. Statistics of natural images: Scaling in the woods. Phys Rev Lett. 1994; 73:814–817. [PubMed: 10057546]

Scholvinck ML, Friston KJ, Rees G. The influence of spontaneous activity on stimulus processing in primary visual cortex. NeuroImage. 2011

Sellers KK, et al. Anesthesia differentially modulates spontaneous network dynamics by cortical area and layer. Journal of neurophysiology. 2013; 110:2739–51. [PubMed: 24047911]

Simoncelli EP, Olshausen BA. Natural image statistics and neural representation. Annu Rev Neurosci. 2001a; 24:1193–216. [PubMed: 11520932]

Simoncelli EP, Olshausen BA. Natural image statistics and neural representation. Annual review of neuroscience. 2001b; 24:1193–1216.

Smyth D, et al. The receptive-field organization of simple cells in primary visual cortex of ferrets under natural scene stimulation. The Journal of neuroscience : the official journal of the Society for Neuroscience. 2003a; 23:4746–59. [PubMed: 12805314]

Smyth D, et al. The receptive-field organization of simple cells in primary visual cortex of ferrets under natural scene stimulation. J Neurosci. 2003b; 23:4746–59. [PubMed: 12805314]

Sohal VS, et al. Parvalbumin neurons and gamma rhythms enhance cortical circuit performance. Nature. 2009; 459:698–702. [PubMed: 19396159]

Steriade M, Amzica F, Nunez A. Cholinergic and noradrenergic modulation of the slow (approximately 0.3 Hz) oscillation in neocortical cells. J Neurophysiol. 1993a; 70:1385–400. [PubMed: 8283204]

Steriade M, McCormick DA, Sejnowski TJ. Thalamocortical oscillations in the sleeping and aroused brain. Science. 1993b; 262:679–85. [PubMed: 8235588]

Tolhurst DJ, Movshon JA, Dean AF. The statistical reliability of signals in single neurons in cat and monkey visual cortex. Vision research. 1983; 23:775–85. [PubMed: 6623937]

Tolhurst DJ, Tadmor Y, Chao T. Amplitude spectra of natural images. Ophthalmic Physiol Opt. 1992; 12:229–32. [PubMed: 1408179]

Tsodyks M, et al. Linking spontaneous activity of single cortical neurons and the underlying functional architecture. Science. 1999; 286:1943–6. [PubMed: 10583955]

Uhlhaas PJ, Singer W. Neuronal dynamics and neuropsychiatric disorders: toward a translational paradigm for dysfunctional large-scale networks. Neuron. 2012; 75:963–80. [PubMed: 22998866]

van der Schaaf A, van Hateren JH. Modelling the power spectra of natural images: statistics and information. Vision Res. 1996; 36:2759–70. [PubMed: 8917763]

van Dijk H, et al. Prestimulus oscillatory activity in the alpha band predicts visual discrimination ability. The Journal of neuroscience : the official journal of the Society for Neuroscience. 2008; 28:1816–23. [PubMed: 18287498]

Vinje WE, Gallant JL. Sparse coding and decorrelation in primary visual cortex during natural vision. Science (New York, NY). 2000; 287:1273–1276.

Voytek B, et al. Shifts in gamma phase-amplitude coupling frequency from theta to alpha over posterior cortex during visual tasks. Front Hum Neurosci. 2010; 4:191. [PubMed: 21060716]

Wang X, et al. Feedforward Excitation and Inhibition Evoke Dual Modes of Firing in the Cat's Visual Thalamus during Naturalistic Viewing. Neuron. 2007; 55:465–478. [PubMed: 17678858]

Weliky M, et al. Coding of Natural Scenes in Primary Visual Cortex. Neuron. 2003; 37:703–718. [PubMed: 12597866]

Whittingstall K, Logothetis NK. Frequency-Band Coupling in Surface EEG Reflects Spiking Activity in Monkey Visual Cortex. Neuron. 2009; 64:281–289. [PubMed: 19874794]

Willmore BDB, Mazer JA, Gallant JL. Sparse coding in striate and extrastriate visual cortex. Journal of Neurophysiology. 2011; 105:2907–2919. [PubMed: 21471391]

Worgotter F, et al. State-dependent receptive-field restructuring in the visual cortex. Nature. 1998; 396:165–8. [PubMed: 9823895]

Zagha E, et al. Motor cortex feedback influences sensory processing by modulating network state. Neuron. 2013; 79:567–78. [PubMed: 23850595]

Highlights

- Bidirectional modulation of oscillations in awake ferrets by naturalistic stimuli.
- Decrease in delta and alpha oscillations correlated with multiunit responses.
- Increase in gamma oscillations correlated with multiunit responses.
- Naturalistic input switched network dynamics in V1 between two distinct states.

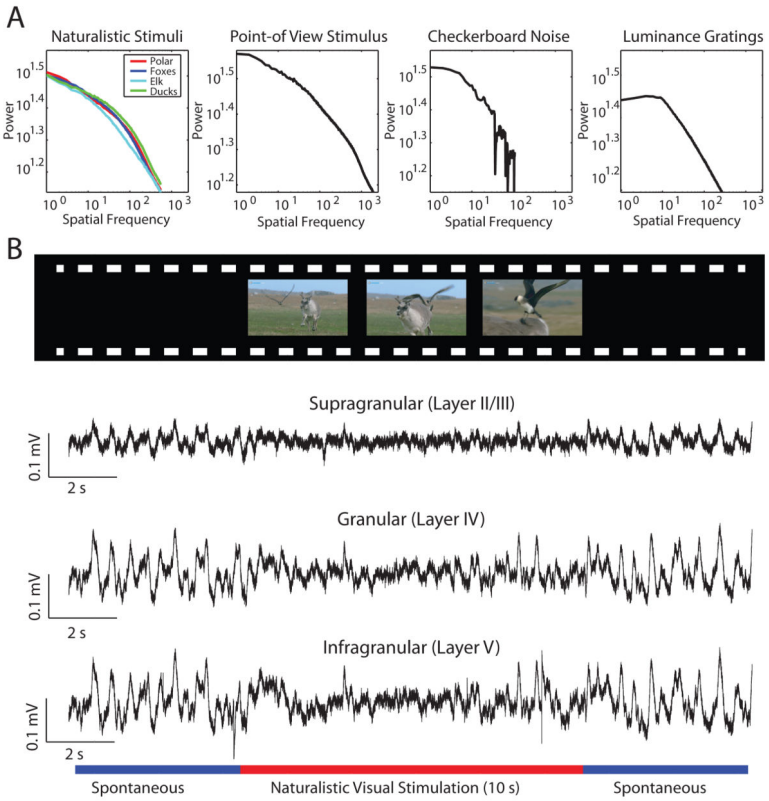

Figure 1. Naturalistic visual stimuli exhibit characteristic spectral properties and modulate LFP dynamics

(A) The spatial frequency of the naturalistic videos used for visual stimulation (far left) and a point-of-view naturalistic image (middle left) exhibit the characteristic 1/f to $1/f^2$ spatial frequency distribution of naturalistic stimuli. Artificial stimuli of black and white checkerboard noise (middle right) and luminance gratings (far right) do not exhibit this spatial frequency structure.

(B) Trials consisted of 10 sec of spontaneous activity (screen dark), followed by 10 sec of naturalistic movie clip, followed by 10 sec of spontaneous activity. Representative local field potential traces simultaneously recorded on electrode contact sites in supragranular (top), granular (middle), and infragranular (bottom) layers of ferret V1.

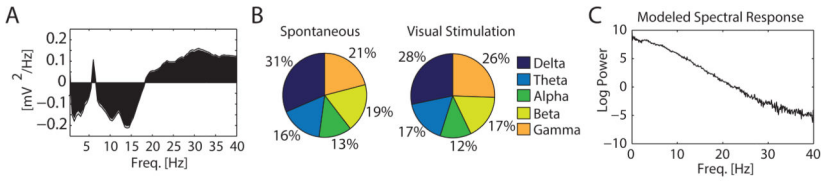

Figure 2. Modulation of mesoscopic network dynamics in V1 by naturalistic visual input during free viewing

(A) Group averaged difference in power spectrum of LFP between spontaneous and visually-evoked activity. Low frequencies exhibited downregulation (with the exception of a small peak in the theta range) and higher frequencies exhibited an upregulation of oscillation power. Gray line indicates ± 1 sem.

(B) Relative power for each frequency band during spontaneous activity (left) and during visual stimulation (right). Relative power was calculated by dividing power in each frequency band by total power, on a trial-by-trial basis. The medians across all trials are plotted.

(C) The LFP spectral modulation is not explained by modeled physiological responses to the naturalistic videos, using spatio-temporal receptive fields characteristic of V1.

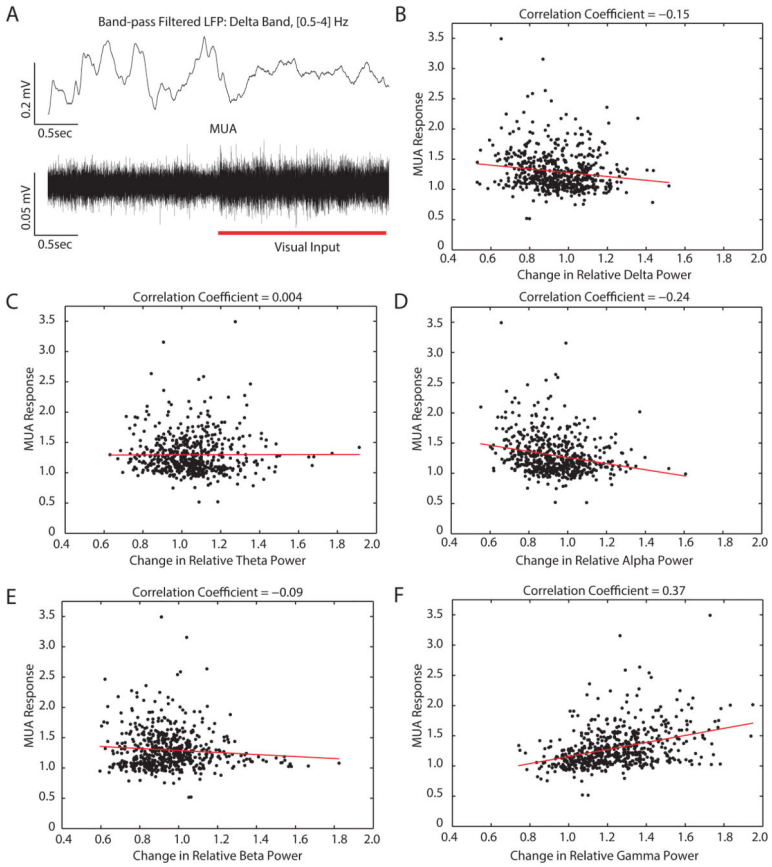

Figure 3. Relationship between mesoscale (LFP) and microscale activity (MUA) during free viewing of naturalistic visual input

(A) Representative sample traces (2 sec of spontaneous activity followed by 2 sec of visual response). Top: band-limited LFP in delta band. Bottom: MUA. Stimulus suppressed power in delta frequency bands and increased MUA.

(B) Enhancement in relative delta power exhibited a negative correlation with enhancement of MUA in response to stimulus. Enhancement in relative delta power was calculated for each trial by dividing the relative power during visual stimulation by the relative power during rest before visual stimulation. MUA enhancement was calculated for each trial by dividing MUA firing rate during visual stimulation by MUA firing rate during spontaneous activity before stimulation. Each data point represents one trial. Best fit line is plotted in red ($y = -0.31x + 1.59$).

(C) Enhancement in relative theta power exhibited a near zero correlation with enhancement of MUA. Each data point represents one trial. Best fit line is plotted in red ($y = 0.007x + 1.29$).

(D) Enhancement in relative alpha power exhibited a negative correlation with enhancement of MUA. Each data point represents one trial. Best fit line is plotted in red ($y = -0.51x + 1.77$).

(E) Enhancement in relative beta power exhibited a near zero negative correlation with enhancement of MUA. Each data point represents one trial. Best fit line is plotted in red ($y = -0.17 + 1.45$).

(F) Enhancement of relative gamma power exhibited a positive correlation with enhancement of MUA. Each data point represents one trial. Best fit line is plotted in red ($y = 0.58x + 0.57$).

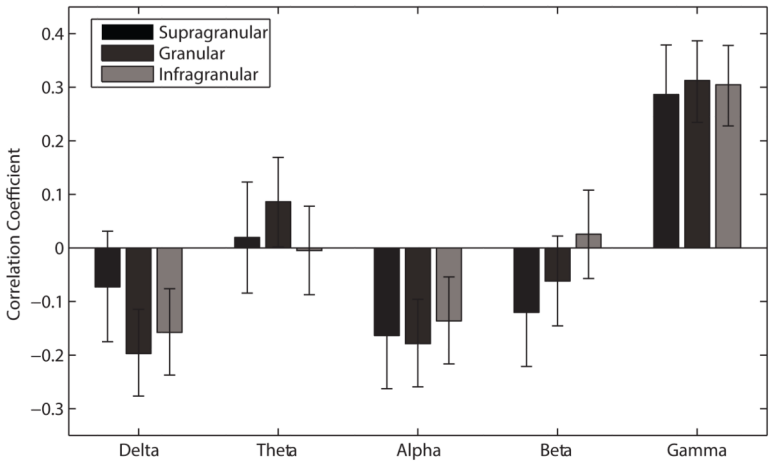

Figure 4.

Relationship between mesoscale (LFP) and microscale activity (MUA) during free viewing of naturalistic visual input as a function of supragranular, granular, and infragranular electrode site locations.

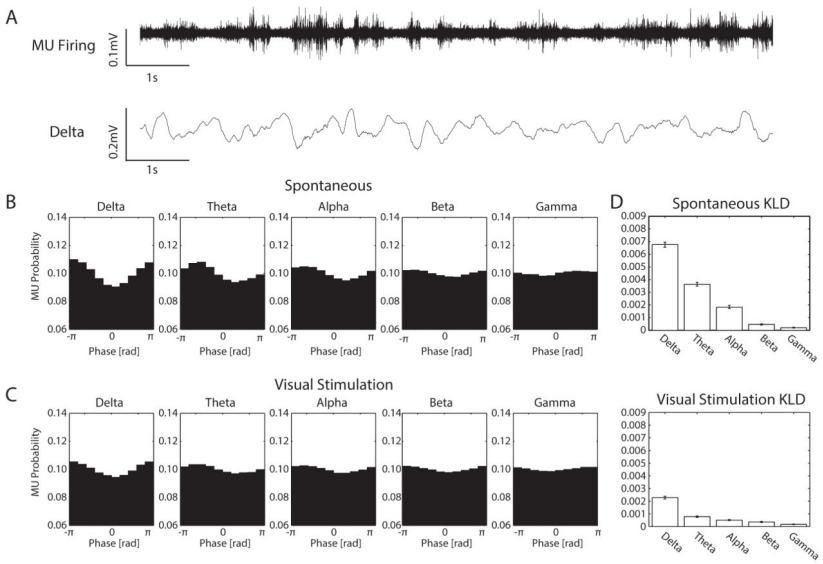

Figure 5. MUA exhibited the strongest preferred phase-of-firing to the delta oscillation; naturalistic visual stimulation decreased MUA preferred phase-of-firing in low frequencies

(A) Simultaneous sample traces during spontaneous activity. High-pass filtered data (top) shows MUA which is phase aligned to the delta phase band-pass filtered LFP (bottom).

(B) Preferred phase-of-firing for all MUA during spontaneous activity, according to the phase of individual frequency bands.

(C) Preferred phase-of-firing for MUA during visual stimulation, according to the phase of each frequency band.

(D) The Kullback-Leibler divergence was used as a metric of non-uniformity of MUA. MUA showed the strongest phase-of-firing preference according to the phase of the delta oscillation. MUA exhibited stronger preferred phase-of-firing during spontaneous activity (top) compared to during visual stimulation (bottom). Plots show median and 95% CI.

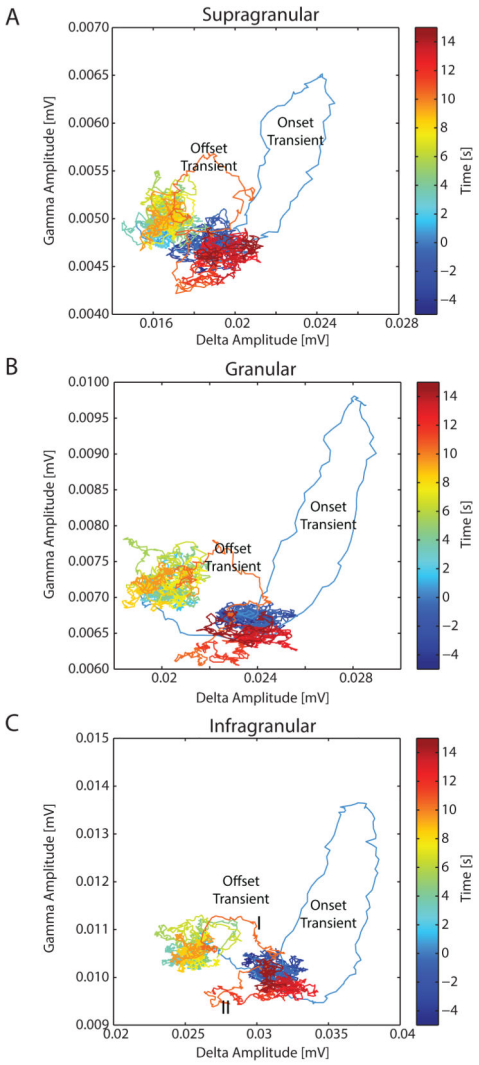

Figure 6. Phase-space representation of instantaneous amplitudes of delta and gamma oscillations

(A) Left: Trajectory of instantaneous delta and gamma amplitudes in supragranular layers, color-coded in 1 second increments. Periods of spontaneous activity are plotted in dark blue (before visual stimulation) and red (after visual stimulation), while periods of visual stimulation are plotted in intermediate colors. Onset and offset of the visual stimulation caused a transient change in both delta and gamma amplitudes.

(B) Same representations as in (A) but for granular layer.

(C) Same representations as in (A) but for infragranular layer.

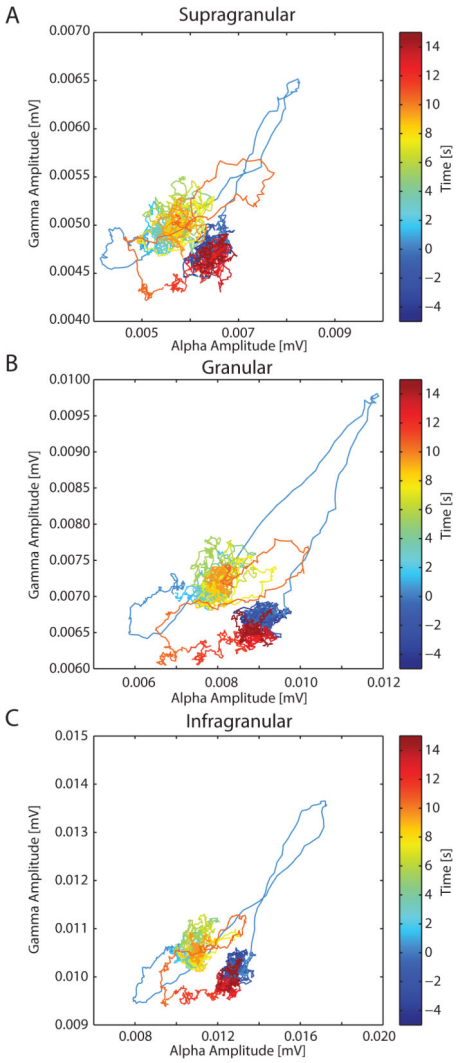

Figure 7. Phase-space representation of instantaneous amplitudes of alpha and gamma oscillations. Same representations as in Figure 6 but for different pair of frequency bands

(A) Left: Trajectory of instantaneous delta and gamma amplitudes in supragranular layers, color-coded in 1 second increments.

(B) Same representations as in (A) but for granular layer.

(C) Same representations as in (A) but for infragranular layer.

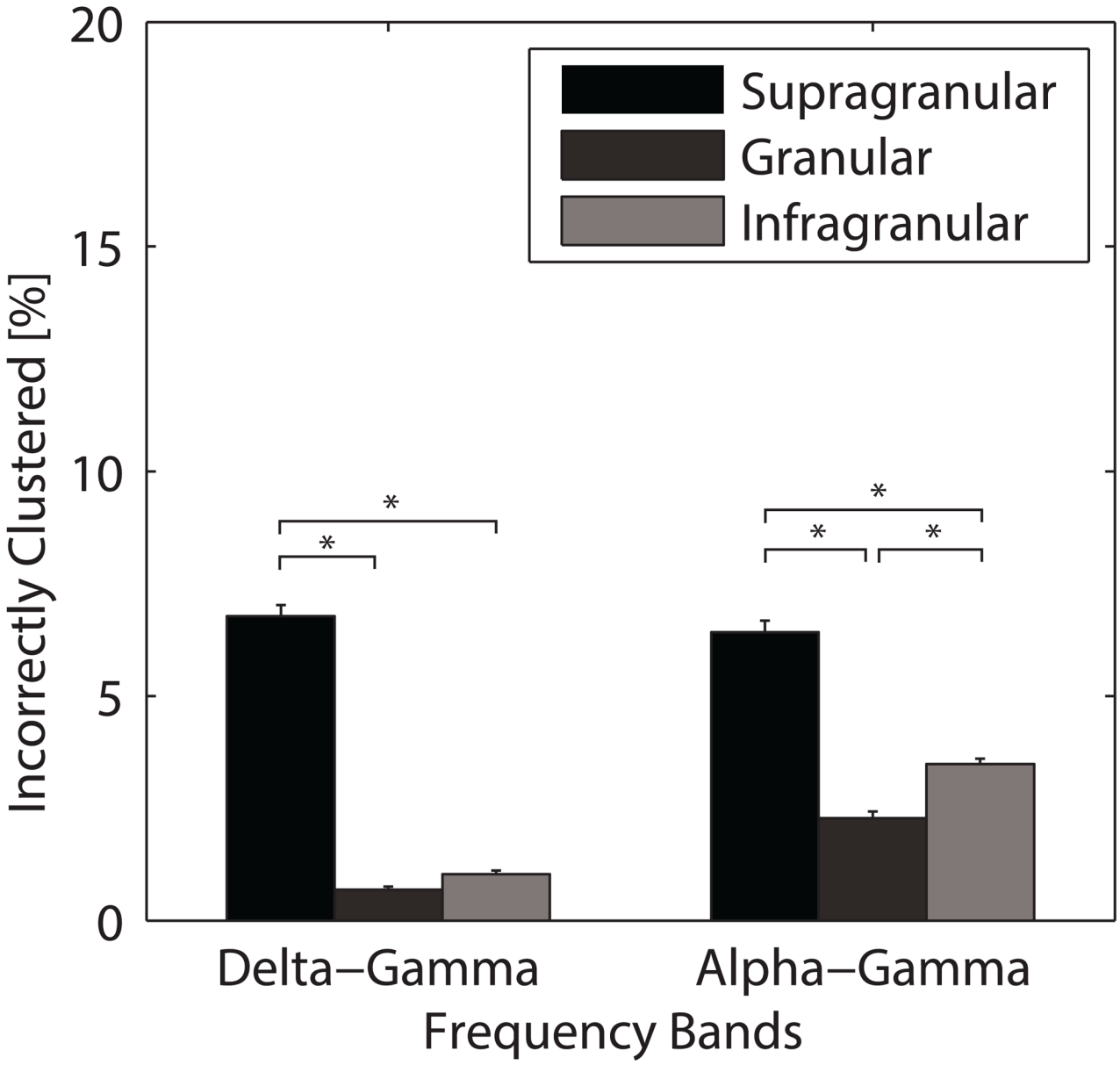

Figure 8.

Percent of incorrectly clustered data points for delta-gamma and alpha-gamma trajectories, respectively. 100 iterations of bootstrapping were conducted to calculate standard error of the mean. Error bars indicate ± 1 sem, * indicates significantly different at $p < 0.05$.

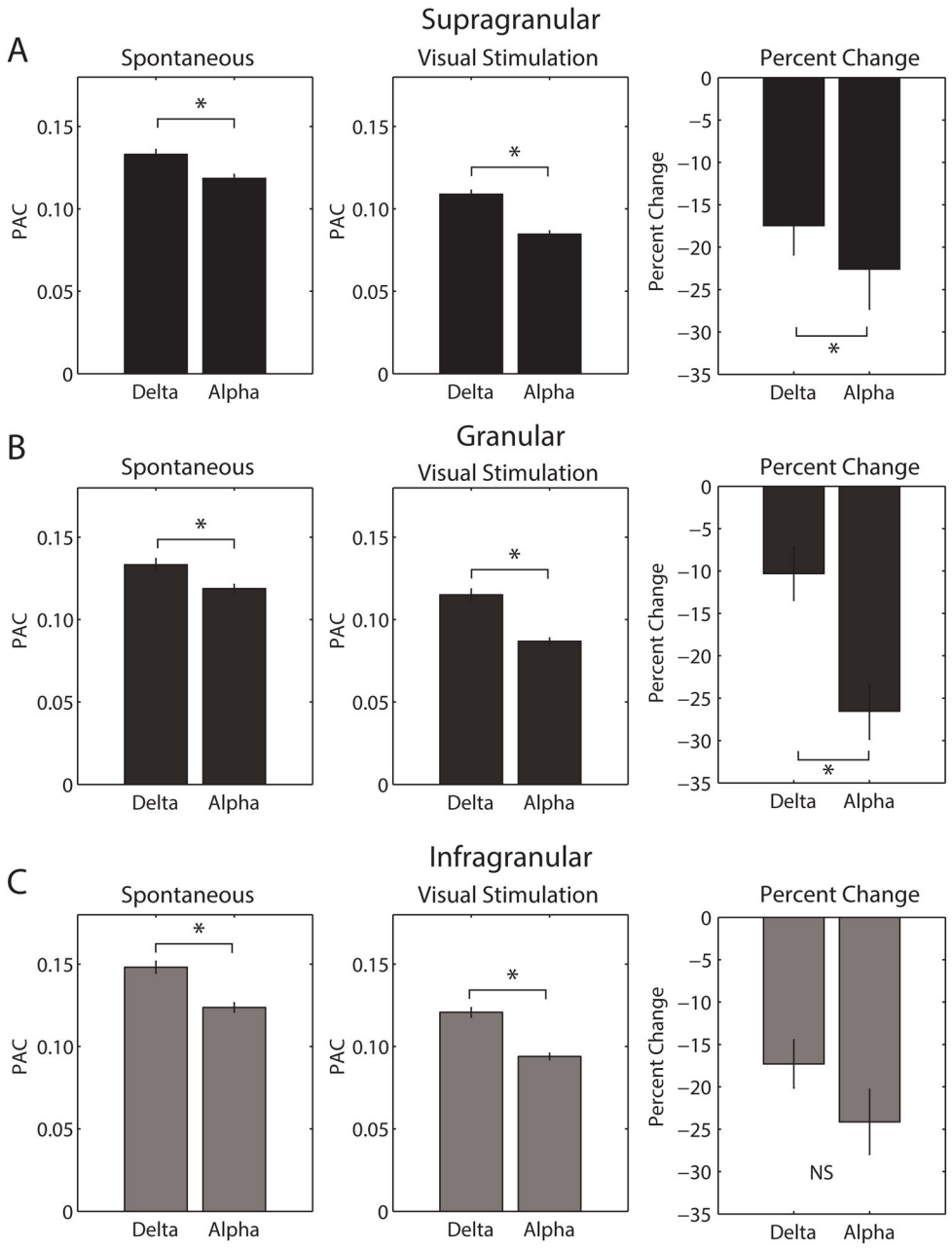

Figure 9. Phase-amplitude coupling (PAC) of low frequency phases and gamma amplitude was decreased by presentation of the naturalistic visual stimulus

(A) PAC during spontaneous activity (left) between delta or alpha phase and gamma amplitude was decreased by presentation of the visual stimulus (middle, right). Coupling between delta phase and gamma amplitude was stronger than alpha-gamma PAC, and was less affected by visual stimulation.

(B) Same representations as in (A) but for granular layer.

(C) Same representations as in (A) but for infragranular layer.